Spring 5-1-2022

Identification of Translesion Synthesis Inhibitors that Target Rev7/Rev3 Protein-Protein Interactions

Seema Patel
seema.patel@uconn.edu

Identification of Translesion Synthesis Inhibitors that Target Rev7/Rev3 Protein-Protein Interactions

Seema Mukund Patel

April 29, 2022

University of Connecticut Honors Program

Department of Molecular and Cell Biology

Thesis Advisor: Dr. M. Kyle Hadden
Honors Advisor: Dr. Charles Giardina
University Scholar Advisory Committee Mentor: Dr. Ashis Basu

Acknowledgments

I would like to thank my research advisor, Dr. Matthew Kyle Hadden, for giving me the opportunity to learn about translesion synthesis and validate drug candidates for anti-cancer properties. I am extremely grateful for his patience, mentorship, and support throughout my undergraduate years. My time working with Dr. Hadden has been an impactful learning experience as he challenged and motivated me to pursue academic achievements that I did not think were possible. His countless revisions of my proposals and positive encouragement made it possible for me to earn distinctions, such as University Scholar and Goldwater Scholar. I would also like to thank my lab colleagues, Anglea Zaino, Radha Charan Dash, Jackson Calhoun, and Noah Harrahill, for guiding me through projects and showing me how to write and present my research effectively. Lastly, I would like to thank my Honors Scholar advisor, Dr. Charles Giardina, and my University Scholar advisory committee mentor, Dr. Ashis Basu, for being invested in my academic career and professional aspirations.

Abstract

Translesion synthesis (TLS) is a specialized mechanism that all cells utilize to replicate past lesions during the S phase. Cancer cells can use TLS to confer DNA damage caused by chemotherapeutics, like cisplatin, by replicating past unrepaired lesions during active replication. This increases the rate of mutations, which leads to the emergence of drug-resistant cancer cells. Preliminary studies have shown that disrupting the protein-protein interactions (PPI) in the TLS heteroprotein complex increases cancer cells' sensitivity to first-line genotoxic chemotherapy, illustrating how inhibiting TLS assembly and function can significantly increase cancer cell death. These results underscore the therapeutic potential of targeting various TLS PPI. This study identifies small molecule inhibitors that disrupt the Rev7/Rev3 PPI with verification of TLS inhibition through biochemical and cellular studies. Our results demonstrate that Rev7/Rev3 TLS inhibitors are not inherently cytotoxic, nor do they have inhibitory effects on cell proliferation and survival in conjunction with cisplatin.

Introduction

Cells are constantly exposed to both endogenous and exogenous DNA damaging agents such as sunlight, ionizing radiation, and chemotherapy. To eliminate these lesions and restore the original DNA sequence, cells utilize various DNA damage repair mechanisms which involve the excision of bases and DNA synthesis (Friedberg, 2003). Despite these highly efficient mechanisms, some lesions may remain unrepaired and interfere with replication through the arrest of replication forks. In such situations, cells use DNA damage tolerance (DDT) mechanisms to bypass these lesions during active replication, without removing or repairing the site of damage. The two primary DDT mechanisms are translesion synthesis (TLS) and template switching. Both processes are commonly used to repair single-strand DNA lesions and homology-dependent repair of double-strand breaks (Dash, 2020). During DDT, the damaged site on the DNA is recognized by the replication machinery, resulting in an arrest that is relieved by TLS.

A diverse set of DNA damaging agents, including platinum-based drugs like cisplatin, are commonly used as first-line chemotherapeutics to treat various types of human cancers, including testicular, breast, head and neck, and ovarian cancers (Brown, 2019). They serve as potent anticancer drugs by chemically modifying the structure of DNA. Cisplatin, for example, creates platinum adducts and crosslinks purine bases which halt replication (Truong, Judy 2019). This triggers cancer cell apoptosis since regular DNA polymerases cannot replicate past these adducts. Prior research has shown that cancer cells can avoid apoptosis by recruiting TLS, where the DNA polymerase is temporarily replaced by specialized, low-fidelity TLS DNA polymerases during active replication (Korzhnev, 2016). Though TLS DNA polymerases prevent genomic instability, they lack exonuclease activity. Moreover, the large active sites of the heteroprotein complex accommodate bulky adducts on the DNA and allow the addition of incorrect nucleotides which potentiates mutagenesis (Dash, 2020). Thus, TLS plays a vital role in decreasing cell sensitivity, increasing cellular resistance to chemotherapeutics, and increasing mutagenesis by leaving lesions unrepaired.

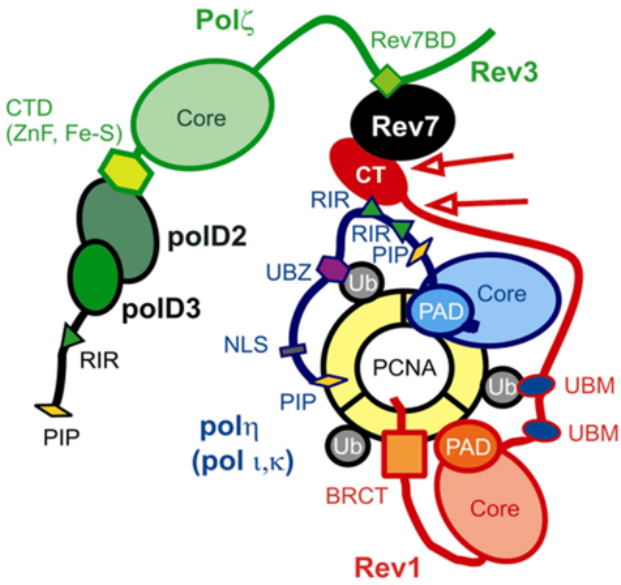

Figure 1: Key Protein-Protein Interactions within the TLS machinery

The TLS machinery comprises five major polymerases: one B-family polymerase polζ and four Y-family polymerases Rev1, polη, polι, and polκ (Korzhnev, 2016). The Y-family polymerases are known as “inserter” polymerases because they insert a nucleotide across the damaged DNA (Dash, 2020). Polζ is referred to as the “extender” polymerase because its primary role is extending the template past the inserted nucleotide; though, polη and polι also can extend in some cases as well (Dash, 2020). As shown in **Figure 1**, polζ is a complex of multiple domains, including the 24-kDa accessory Rev7 and 350-kDa catalytic Rev3 subunit (Pustovalova, 2012). Both subunits function in conjunction since Rev3 is required for Rev7 to dimerize and therefore be functional in

the TLS pathway (Rizzo, 2018). Rev1 has a unique C-terminal domain that binds and recruits the other four essential TLS polymerases on proliferating cell nuclear antigen (PCNA), thereby coordinating the entire TLS pathway; this is known as the Rev1 bridge mechanism. Specifically, when a replicative polymerase, such as polδ, encounters and stalls at the site of DNA damage, it triggers a cascade of events that initiate TLS. The stalling leads to the monoubiquitination of PCNA (UbPCNA) which facilitates the localization of Rev1 to the stalled replication forks. Rev1 interacts with UbPCNA and recruits inserter polymerases via its C-terminal domain (**Figure 2** from Dash, 2020). Extensive research has shown that Rev1 mutants lacking the C-terminal domain experience increased cellular sensitivity to DNA damage and have reduced mutation rates, thereby highlighting the essential role of Rev1/polζ protein-protein interactions (PPI) in TLS assembly (Pustovalova, 2012).

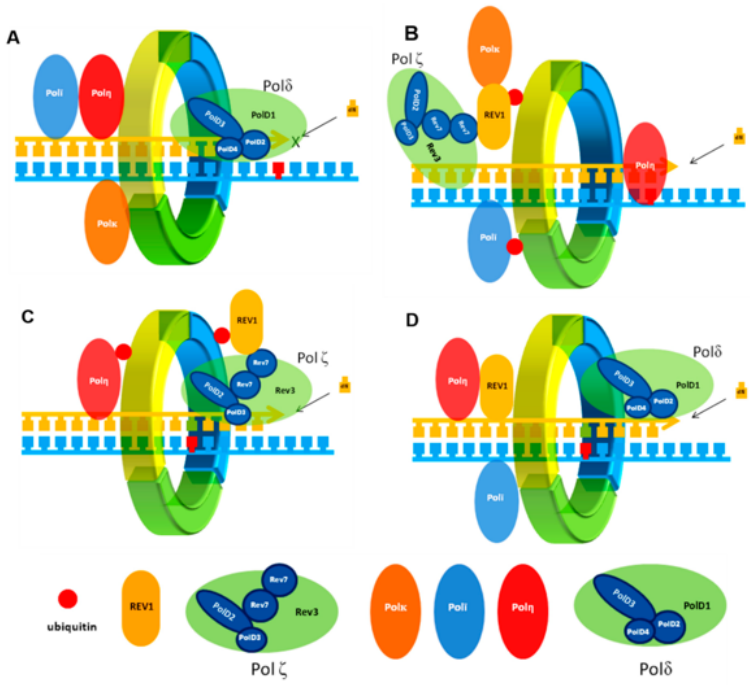

Figure 2: Mechanism of TLS in eukaryotes

Targeting Rev7 and Rev3 are of interest because they play an important role in preventing cisplatin cytotoxicity. Human fibroblasts expressing reduced levels of Rev3 are more sensitive to cisplatin and loss of Rev3 function greatly increases mutagenesis in response to DNA damaging agents, such as UV light and benzo(*a*)pyrene diol epoxide (Wu, 2004, Gan 2008). The effects of Rev3 suppression have also been evaluated in preclinical settings. A 2010 study by Doles et al. examined the impact of Rev3 depletion in cisplatin response in a chemoresistant mouse model of late-stage lung adenocarcinoma. The study demonstrated tumor regression or growth stasis in cisplatin-treated, Rev3-knockdown mice transplants and an overall extension of survival in Rev3-deficient mice (Doles, 2010).

Rev7 (also known as MAD2L2 and MAD2B) is a multifunctional protein involved in TLS, DNA repair, cell cycle regulation, and histone modification. Like Rev3, Rev7 is necessary to bypass cisplatin-induced DNA damage (Sakurai, 2020). The reduction of Rev7 using siRNA in human fibroblasts increases UV sensitivity and decreases UV-induced mutagenesis, indicating Rev7 engages in DNA damage tolerance and damage-induced mutagenesis (McNally, 2008). A 2020 study by Sakurai et al. demonstrated that decreased expression of Rev7 enhances chemosensitivity, restores cisplatin resistance, and upregulates apoptosis-associated genes in testicular germ cell tumors, suggesting Rev7 may be a potential therapeutic target in chemoresistant testicular cancer (Sakurai, 2020).

These studies underscore the therapeutic potential of targeting the Rev7/Rev3 PPI to sensitize cancer cells to already existing DNA damaging agents in the market. Despite these promising results, more progress needs to be made to develop novel and potent Rev7/Rev3

inhibitors. As shown in **Figure 3**, a 2016 study by Actis et al. identified “Compound 7” as an inhibitor of the interaction between Rev7 and the Rev7 binding sequence, Rev3L (Actis, 2016). Clonogenic survival of HeLa cells treated with cisplatin and Compound 7 was lower than that of cells treated with cisplatin alone, indicating Compound 7 behaves in a manner expected of a TLS inhibitor (Actis, 2016). My thesis identifies three more Rev7/Rev3 inhibitors and tests their inhibitory effects using the first optimized *in vitro* biochemical assay. These three inhibitors were also tested in combination therapy with cisplatin to evaluate their efficacy against specific ovarian cancer cell models.

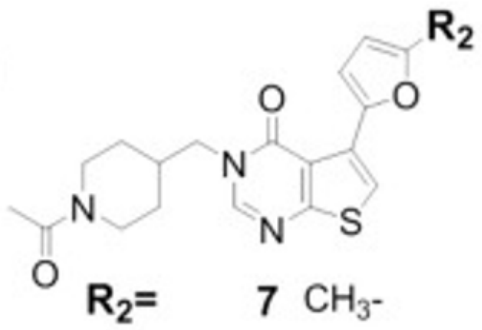

Figure 3: Structure of Compound 7

Methods

I. Molecular Dynamics Studies to Probe the REV7/RBM Interaction

To determine the key amino acid residues/minimal binding motif from Rev3 necessary to bind with Rev7 (RBM), molecular dynamics studies were performed. Structures of Rev7 complexed with two RBMs were deposited in the RCSB database. As shown in **Figure 4**, the RBMs evaluated include RBM1 (Rev3 residues 1875-1896) and RBM2 (Rev3 residues 1991-2012). The computational analysis displayed varying conformational structures (α-helices and β-strands) when Rev7 was complexed with either of the two RBMs. Verifying the structural properties of the complex is important to assure that Rev7 is in its closed, “safety belt” conformation.

Using the Maestro program by Schrödinger, time-dependent molecular dynamic stability analyses were performed for each Rev7/RBM complex. Molecular dynamics studies allow us to analyze the physical movements of atoms within the complex for a fixed period of time (50 nanoseconds), giving a glimpse of the dynamic interactions taking place in the system. Crystal structures of the Rev7/RBM complex were used as a reference frame to calculate the root mean square deviation of Rev7 which quantifies the movement/stability of Rev7 atoms when complexed with RBM. Next, to better understand binding energetics for each amino acid involved in the Rev7/RBM complexes, we performed a binding free energy analysis to calculate ΔH^d, the total enthalpy of the system, as well as the per-residue binding free energy.

II. Fluorescence Polarization (FP) Assay Optimization

For the FP assay, a fluorescein amidite (FAM) label was covalently linked to the N-terminus of a human RBM1 peptide. The FAM-RBM1 peptide forms a stable 1:1 complex with full-length, unlabeled human Rev7. 10 µL of a 0.2 µM solution of FAM-RBM1:Rev7 peptide complex (purchased from Genscript) diluted in phosphate-buffered saline (PBS) was added to a black 384-well plate. Either unlabeled RBM1 or RBM2 (10 µL, varying concentrations) were added to the wells with the complex to give final concentrations of 100 µM − 1 nM in a total volume of 20 µL/well. In each plate, the negative control was 20 µL PBS and the positive control was 10 µL of 0.2 µM complex with 10 µL of 0.2 µM unlabeled RBM2. The plate was incubated at room temperature for 1 hour with gentle mixing. Fluorescence polarization was measured in millipolarization units on a Synergy H1 Hybrid multimode microplate reader (Biotek, excitation

485 nM, emission 528 nM) at 15, 30, 60, 90, and 120 minutes. The IC50 values — the concentration of unlabeled RBM required for 50% displacement of the FAM-RBM1:Rev7 peptide complex — were determined by creating a nonlinear regression of the data for log concentration vs. response on GraphPad Prism 5.

III. Virtual Screening Using a Receptor-Based Docking Model

To identify small-molecule inhibitors that disrupt the Rev7/Rev3 PPI through direct binding with a defined pocket on Rev7, we performed a high-throughput virtual screen (HTVS) of compounds from our in-house ChemBridge library. The structures of Rev7 and Rev3 were uploaded on Schrödinger, a computer software system, and compounds that had the greatest binding affinity to Rev7 were selected. From the HTVS protocol, compounds with a predicted docking score ≤ −6.0 were subjected to the more rigorous Glide standard precision (SP) procedure, which docks thousands of ligands with high accuracy. Compounds that exhibited an SP Glide score < −8.0 were docked with Rev7 in Glide extra precision (XP) mode. XP mode is the most robust docking procedure that further eliminates false positives through extensive sampling and advanced scoring, resulting in higher enrichment of ligands that fits within the Rev7 domain. This led to the identification of 31 hit compounds (XP Glide score ≤ −9.0), of which 9 compounds with XP Glide score ≤ -8.0 were further evaluated. (**Figure 6**)

IV. Validation of Hit Compounds using FP Assay

For the pilot screen, each of the 9 hit compounds was diluted in PBS to give final concentrations of 100 μM − 1 nM in a total volume of 20 μL/well. Compounds (10 μL) and FAM-RBM1:Rev7 complex (10 μL, 0.2 μM) were mixed and incubated in 384-well black plates at room temperature for 1 hour. In each plate, the negative controls were 20 μL of PBS and 20 μL of the 0.2 μM complex alone. The positive control was 10 μL of the 0.2 μM complex with 10 μL of 0.2 μM RBM2. Fluorescence polarization and IC50 values were measured as described above. All graphs and statistical analyses were conducted using GraphPad Prism 5.

V. MTS Cell Proliferation Assay

To perform this assay, wash both cell lines (A2780 and A2780cisR) with 5 mL of PBS (Gibco), aspirate the PBS, and add 3 mL of 0.25% 1X Trypsin-EDTA (Gibco) to detach the cells from the surface of the flask. Centrifuge the cells in 5 mL of RPMI-1640 growth media, aspirate the supernatant, and resuspend the cell pellet in 5 mL of media. To count the cells, prepare a 1:1 dilution of 10 μL suspended cells and 10 μL 0.4% Trypan Blue stain (Invitrogen). From the cell count, seed approximately 20,000 cells per 100 μL of growth medium in a 96-well plate. The control wells contain only 100 uL of growth medium to obtain a value for background luminescence. The vehicle control was treated with 1 μL of DMSO to account for the DMSO used to prepare dilutions of Rev7/Rev3 inhibitors. After an incubation period of 24 hours at 37°C, drug the cells with their respective compounds. There are 4 treatment groups: 2 μL of cisplatin at 250, 200, 100, 50, 25, 10, 5, 1, and 0.2 μM added alone, 2 μL of Rev7/Rev3 inhibitor at the above concentrations added alone, and 1 uL of 10 μM and 5 μM cisplatin added to the same varying concentrations of the inhibitor. Once the wells are drugged, incubate the cells for 48 hours at 37°C. 20 μL of a 20:1 MTS Reagent Powder (Promega) and phenazine methosulfate (Sigma) mixture were added to each well and incubated at 37°C for 2 hours. The

absorbance of each well was measured at 490 nm using a Biotek Synergy H1 Hybrid multimode microplate reader and these values were used to calculate the percent viability to determine the GI50 (the concentration for 50% of maximal inhibition of cell proliferation) of each treatment.

Note: To maintain cisplatin resistance in the A2780cisR cell line, add 1% cisplatin (Sigma) to the flask after every third passage. Both cell lines should be cultured at 37°C in RPMI-1640 (Gibco) growth media containing 2mM glutamine, 10% fetal bovine serum, and 1% penicillin-streptomycin (Gibco).

Results

I. Molecular Dynamics Studies to Probe the REV7/RBM Interaction

The docking study was performed to inform our virtual screen. We sought to identify the essential amino acids from Rev3 that bind to Rev7 to keep the Rev7/Rev3 PPI intact. This information was then used to screen compounds with the greatest binding affinity. From the docking study, we observed that both RBM peptides contain three primary regions: βRBM which forms an antiparallel β-sheet ($RBM1_{REV3}$:I1877–P1880, $RBM2_{REV3}$:K1990–P1996), a proline core region ($RBM1_{REV3}$:L1881–P1885, $RBM2_{REV3}$:C1997–P2001), and an α-helix binding region ($RBM1_{REV3}$:S1886–A1892, $RBM2_{REV3}$:S2002–A2012). (**Figure 4**) Sequence alignment studies of the RBM1 and RBM2 peptides suggest that the sequence, φφxPxxxxP could represent the minimal sequence required for Rev7 recognition, where φ represents an aliphatic residue, x represents any amino acid, and P represents proline. Further studies showed that the proline core of both RBM peptides is sufficient to recognize the Rev7 binding site whereas the α-helix region provides an additional contact surface for better binding affinity to Rev7. For the virtual screen, compounds were docked against the βRBM region because it was predicted to have the strongest binding interactions.

When Rev7 was complexed with both RBM peptides to study conformational changes, RBM1's RMSD value was 2.0 Å while RBM2 had an RMSD value of 1.93 Å, suggesting that the Rev7 structure remained relatively stable in the bound state despite multiple rotational bonds and extended peptide length. There was also no change in the orientation of the RBM peptides in the Rev7 binding site throughout the simulation period.

Figure 4: Sequence alignment of the RBM peptides that were subsequently used to perform the virtual screen and synthesize the FAM-labeled complex used in the FP assay. βRBM - yellow, proline core - green, and αRBM - blue.

II. Fluorescence Polarization Optimization

With the help of a postdoctoral researcher in the Hadden Laboratory, we performed docking studies to identify the shortest peptide sequence needed to disrupt the Rev7/Rev3 PPI. This was done through a series of computational work involving time-dependent molecular dynamic studies and binding free energy calculations. Conformation stability of both Rev7 binding motifs (RBM) and Rev7 was studied and validated with experimental IC50 values. (**Table 1**)

RBM	IC50 (μM)	ΔH^d (kcal/mol)
$RBM1_{REV3}$	1.9 ± 0.7	-561.16 ± 48.9
$RBM2_{REV3}$	2.1 ± 0.6	-756.34 ± 33.8

Table 1: Half maximal inhibitory concentration (IC50) and total enthalpy for the REV7:RBM complexes

We developed an FP assay to determine which RBM peptide best disrupts the Rev7/Rev3 PPI and optimize experimental parameters (time and complex concentration) so that we can subsequently verify results from our virtual screen in a biochemical assay. To determine the optimal concentration of the FAM-RBM:Rev7 complex to use in the FP assay, we evaluated the ability of unlabeled RBM peptides (across a wide range of concentrations) to disrupt the FAM-labeled complex at various time points. As shown in **Figure 5**, when both the unlabeled RBM1 or RBM2 peptide concentrations were greater than 0.2 μM, the changes in fluorescence polarization (measured in mP units) upon displacement of the FAM-labeled complex with the unlabeled RBM peptide were modest. Though the IC50 values in **Table 1** are not statistically significant from each other, we chose RBM1 for our subsequent screen because it exhibits a slightly greater binding affinity for Rev7 than RBM2, suggesting a more stable complex for assay development. This decision was also informed by the FP assay optimization data shown below which demonstrates that the assay was most reproducible when the unlabeled RBM1 peptide concentration was 0.2 μM with an incubation time of 60 minutes; therefore, we utilized this concentration and time for the remainder of our FP assays (**Table 2**). For subsequent hit validation FP assays, the negative control was 20 μL PBS and the positive control was 10 μL of 0.2 μM FAM-complex with 10 μL of 0.2 μM unlabeled RBM2.

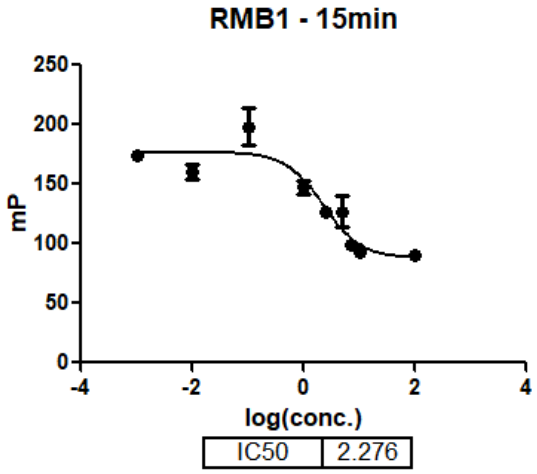

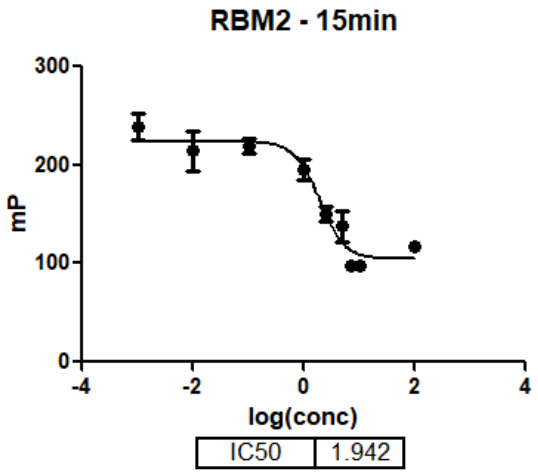

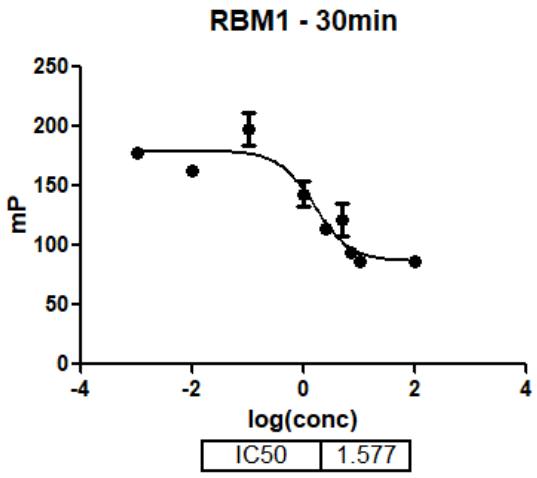
RBM1 - 30min
mP
log(conc)
IC50 1.577

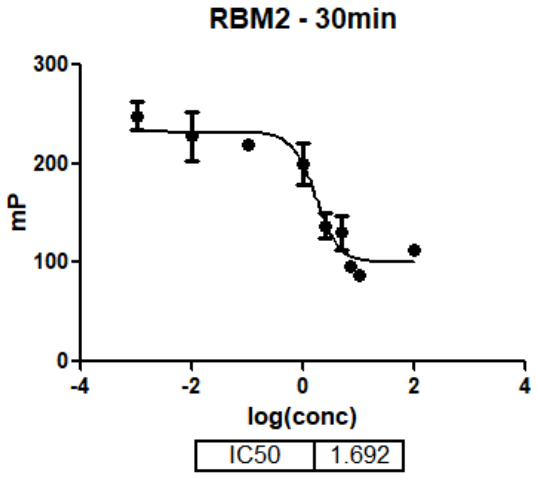
RBM2 - 30min
mP
log(conc)
IC50 1.692

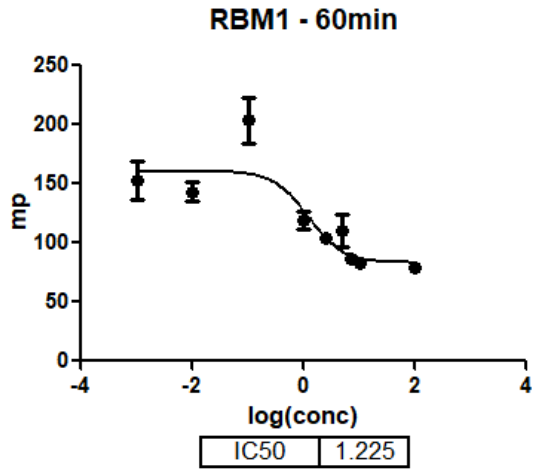
RBM1 - 60min
mp
log(conc)
IC50 1.225

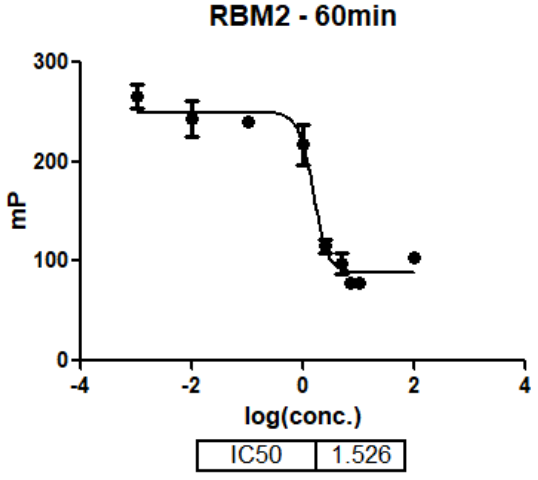
RBM2 - 60min
mP
log(conc.)
IC50 1.526

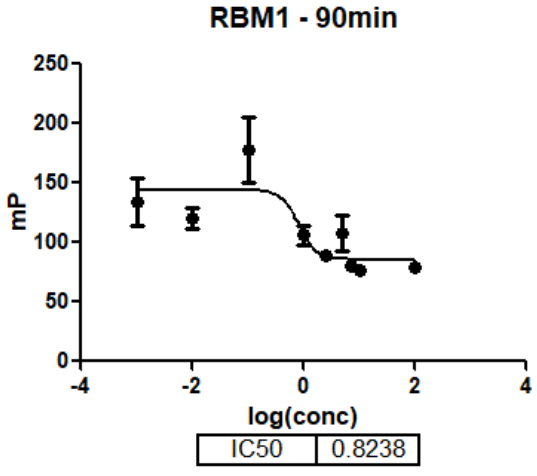
RBM1 - 90min
mP
log(conc)
IC50 0.8238

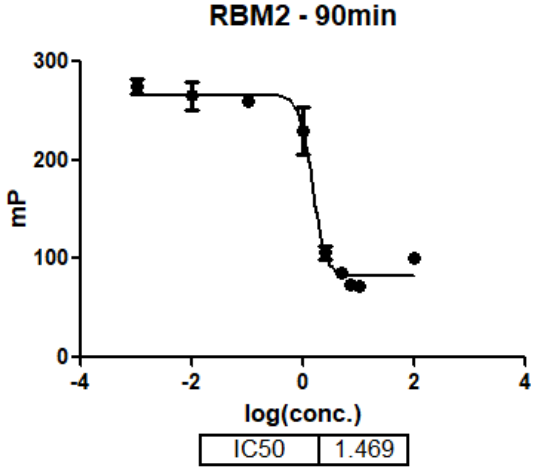
RBM2 - 90min
mP
log(conc.)
IC50 1.469

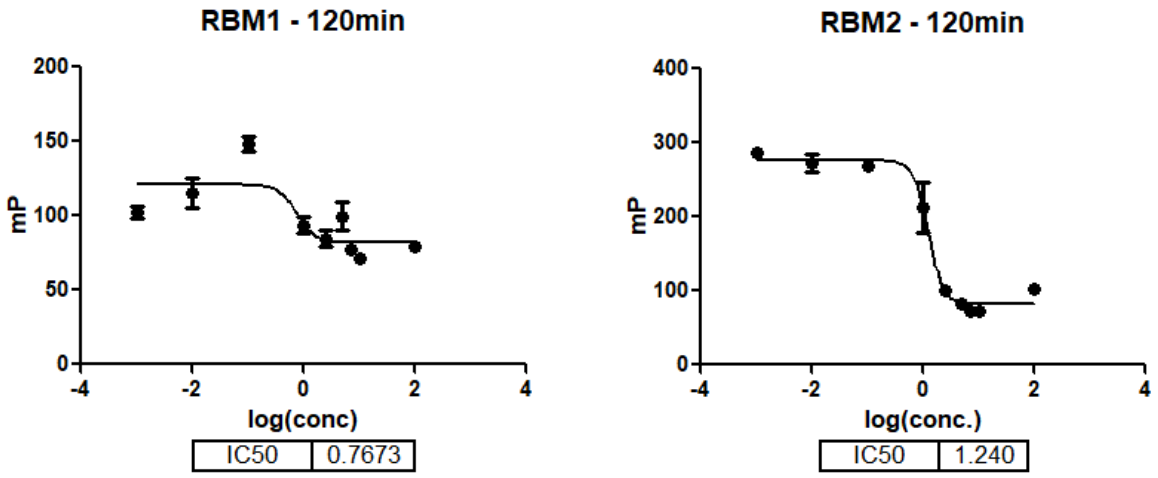

Figure 5: Optimization of FP assay parameters (incubation time and unlabeled RBM concentration). Time-course experiments for the displacement of FAM-RBM1 from Rev7 with unlabeled RBM1 and unlabeled RBM2. IC50 values for each of these time points were calculated through nonlinear regression in GraphPad Prism.

Time (minutes)	RBM1 (μM)	RBM2 (μM)
15	2.276	1.942
30	1.577 ± 0.429	1.692 ± 0.574
60	1.308 ± 0.644	1.526 ± 0.405
90	0.824	1.469
120	0.727	1.240

Table 2: Summary of FP assay data for RBM1 and RBM2, with IC50 values and standard deviation at different time points. Based on the initial data, a second trial was only performed for time points, 30 and 60 minutes.

III. Virtual Screen

Virtual screening is a common, receptor-based computational method used in drug discovery to screen libraries of compounds that can best bind to a target protein of known structure. It is optimized to produce an output of a few compounds that can be easily synthesized or purchased and tested. From the initial screen of our in-house library of 155,155 compounds, we identified 9 hit compounds that had the best binding affinity to the Rev7/Rev3 PPI (**Figure 6**). Based on the FP assay data of compounds from the initial screen, a second virtual screen was performed to compare these promising hits to the rest of the library and identify pharmacophore derivatives of Compound A.

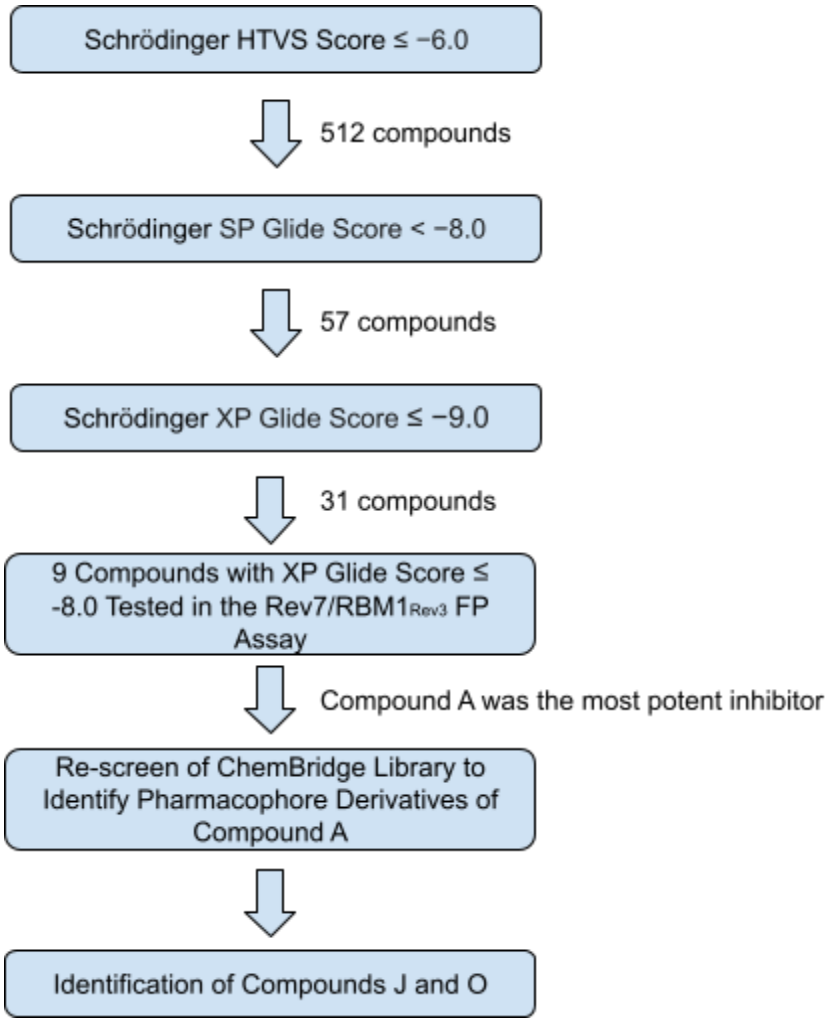

Figure 6: Workflow for computational screening and hit identification

IV. Hit Compound Validation using FP Assay

The optimized FP assay serves as a biochemical experiment to verify if the hit compounds from the virtual screen disrupt Rev7/Rev3 PPI *in vitro*. In the FP assay, the polarization value is expressed in millipolarization (mP) units. The degree of polarization is inversely related to the molecular rotation of the complex. Therefore, a small molecule like the FAM-labeled RBM1 peptide will tumble more rapidly when freely floating than when it is bound to Rev7. A high mP value denotes that the Rev7/Rev3 PPI are intact while a low mP value means that the small molecule inhibitor was successful at disrupting the PPI. A clear drop in polarization means compounds bind to the target protein sequence and have potential TLS inhibitory effects.

From the initial virtual screen, 9 of the 31 compounds identified as potential hits were evaluated for their ability to disrupt the Rev7/Rev3 PPI using the FP assay. Only Compound A had the most inhibitory potential (IC50 13.25 ± 6.86 μM) and was classified as our primary hit. (**Figure 7**) Next, we performed a similarity search of Compound A to identify pharmacophore derivatives and study structure-activity relationships. As shown in **Figure 8**, Compounds J (IC50 8.05 ± 3.42 μM) and O (IC50 4.00 ± 4.41 μM) also successfully displaced the FAM-labeled

complex, thus showcasing the ability to disrupt the Rev7/Rev3 PPI. Compounds A, J, and O are all structurally similar, containing 2 hydrophobic scaffolds connected by a hydrophilic amide linker. (**Figure 9**)

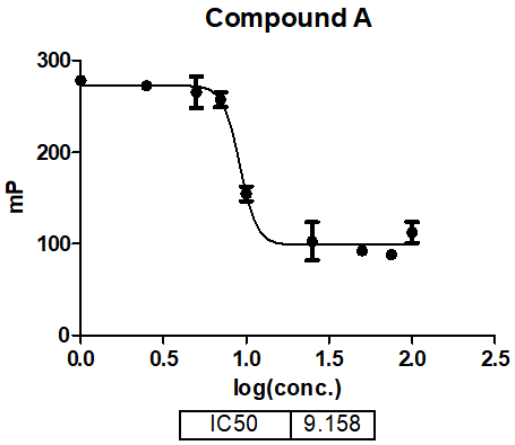

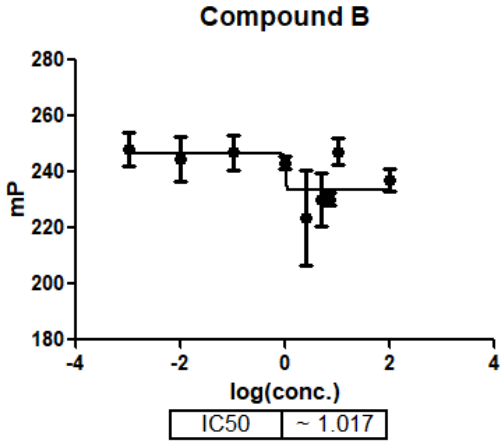

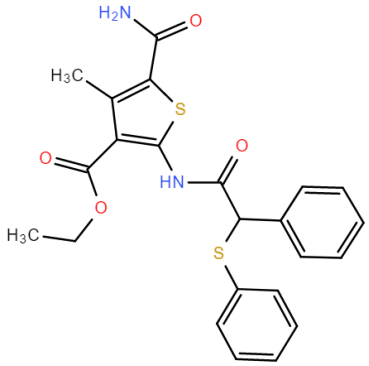

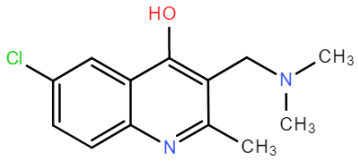

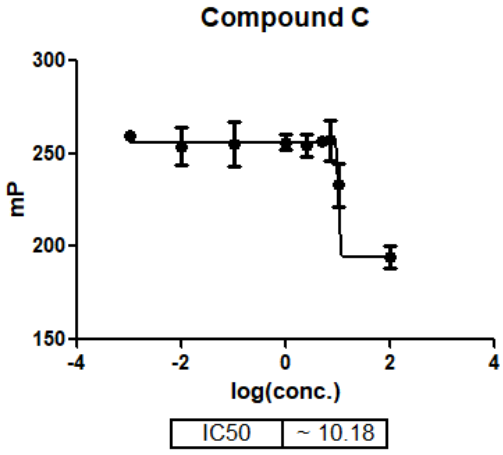

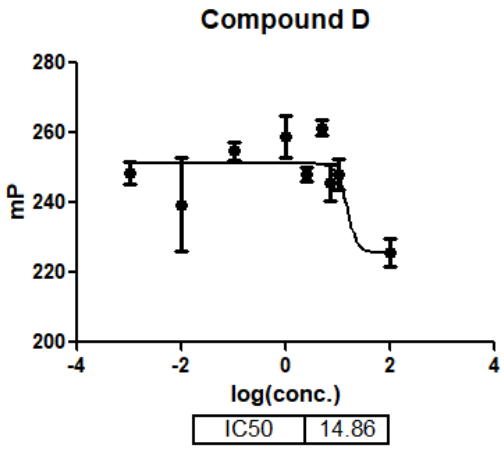

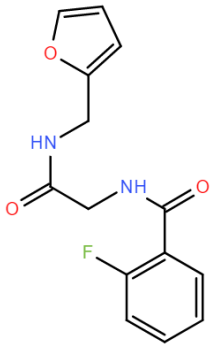

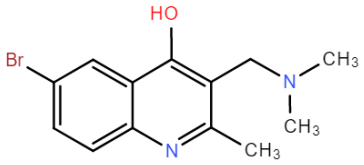

Compound E

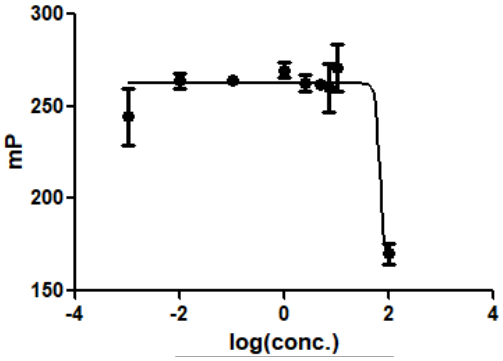

Compound F

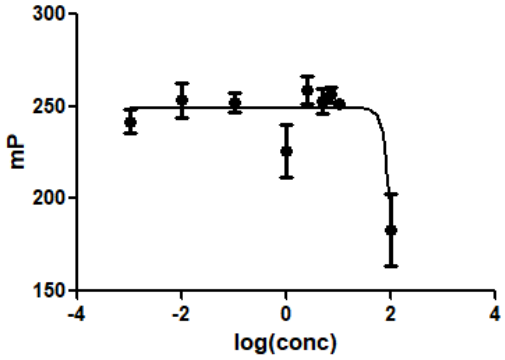

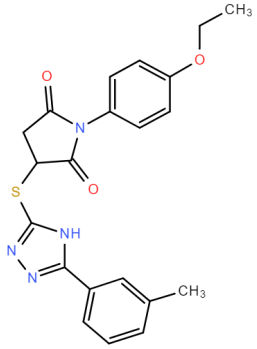

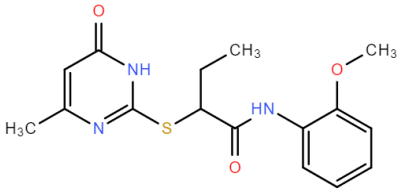

Compound G

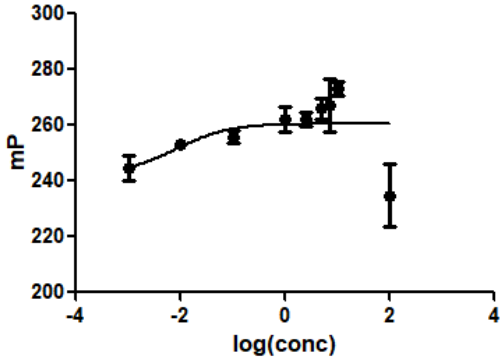

Compound H

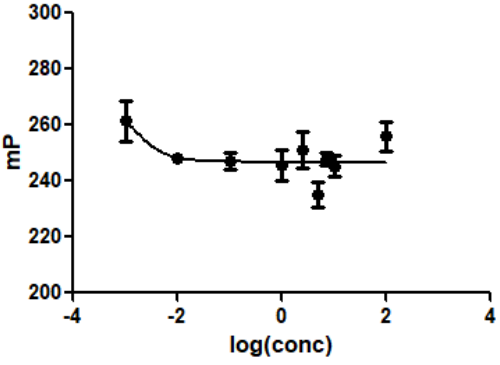

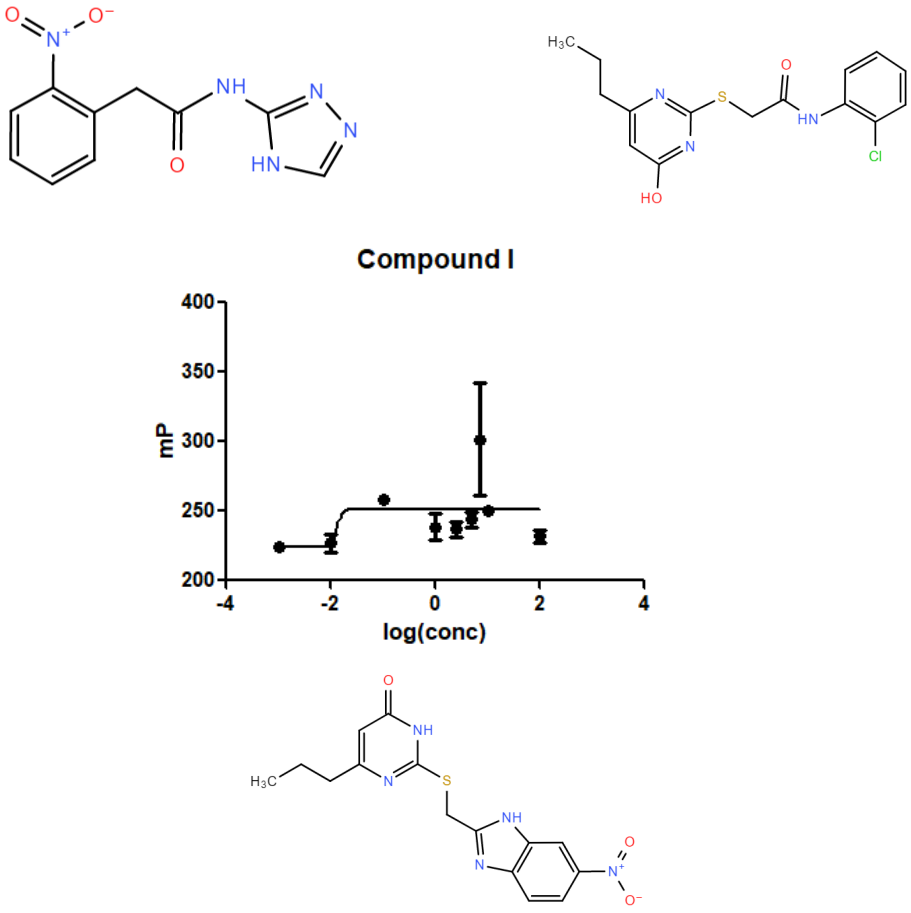

Figure 7: Concentration-dependent disruption of the Rev7/RBM1$_{Rev3}$ PPI by hits from the initial screen. The graphs above are from a representative experiment performed in triplicate. The structure of the compounds is below their respective graphs. IC50 values were calculated through nonlinear regression in GraphPad Prism.

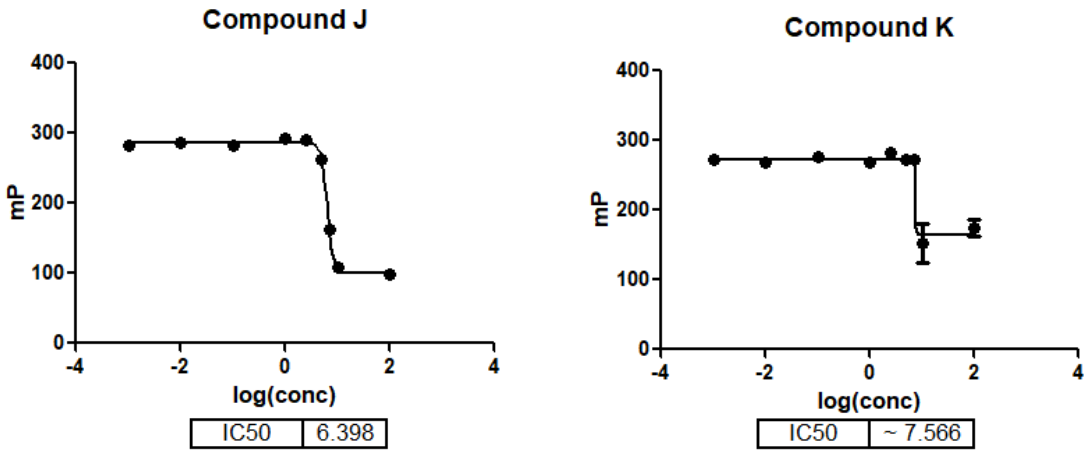

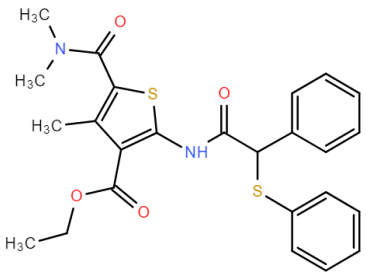

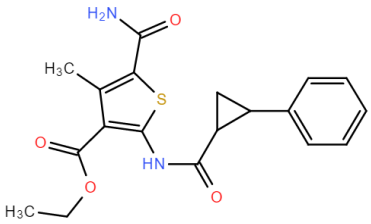

Compound L

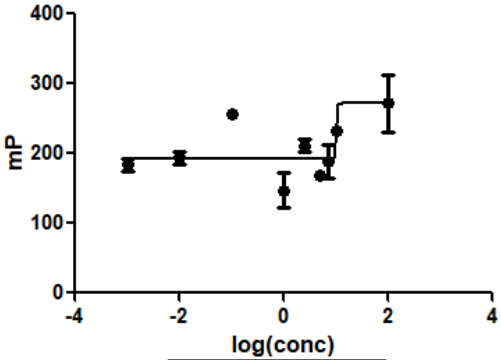

Compound M

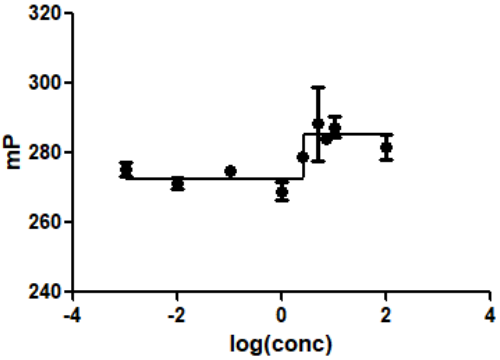

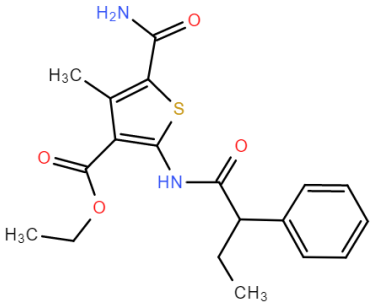

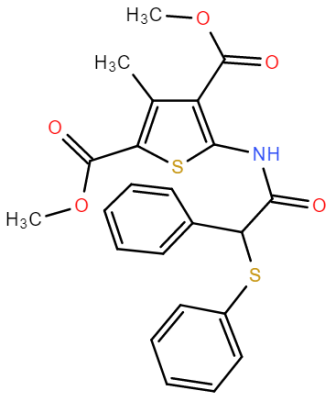

Compound N

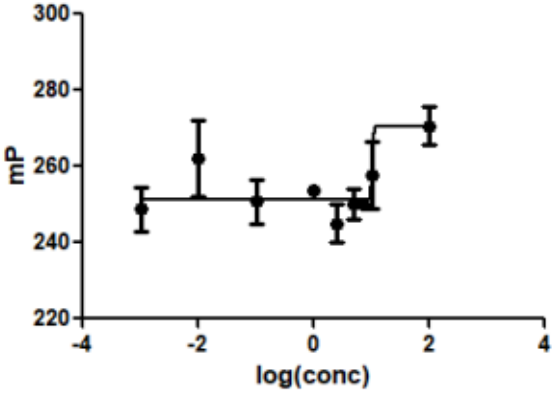

Compound O

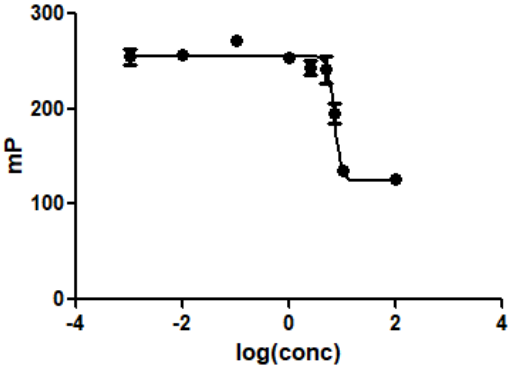

IC50	7.124

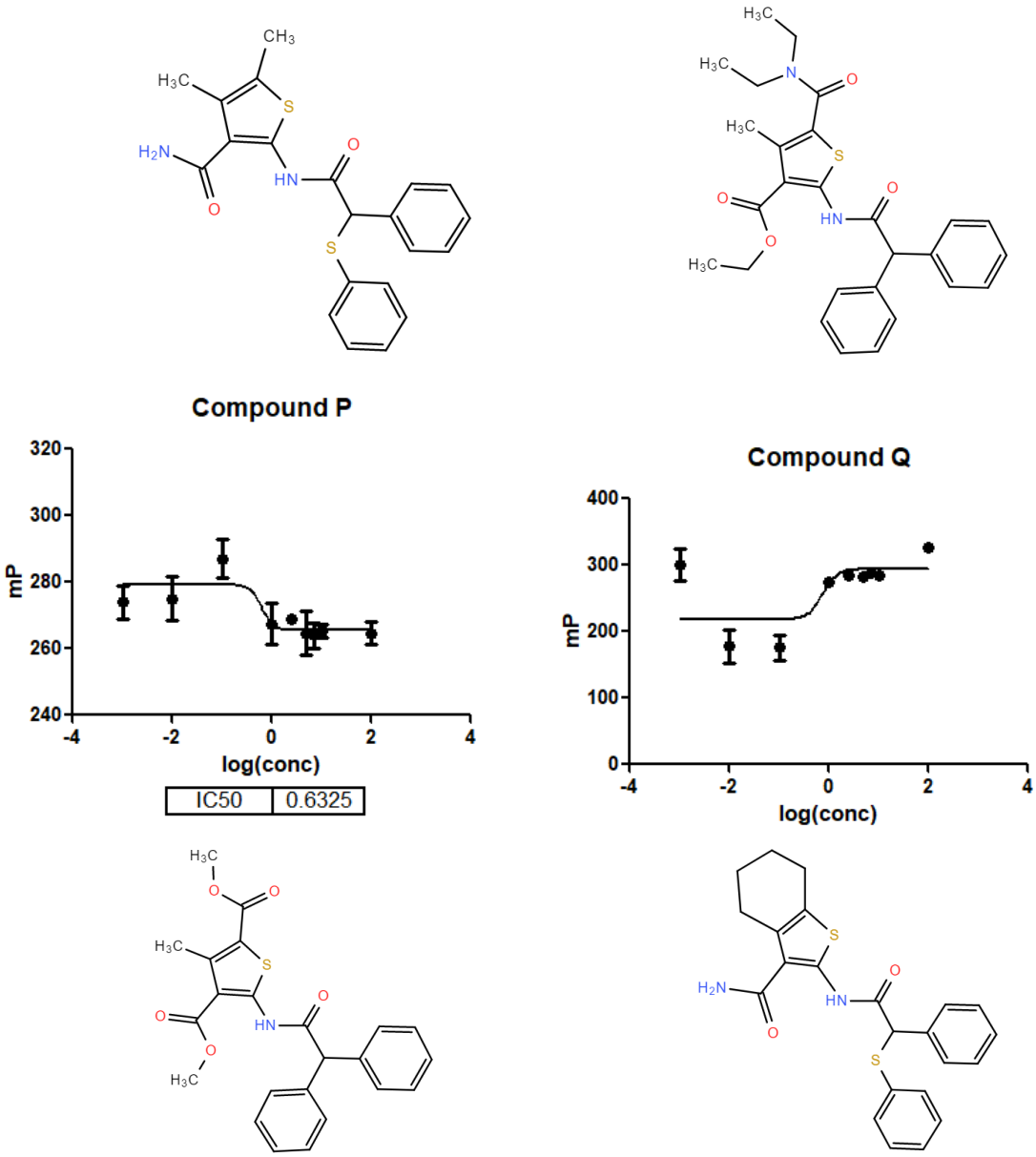

Figure 8: Concentration-dependent disruption of the Rev7/RBM2$_{Rev3}$ PPI by hits from the similarity search to Compound A. The graphs above are from a representative experiment performed in triplicate. The structure of the compounds is below their respective graphs. IC50 values were calculated through nonlinear regression in GraphPad Prism.

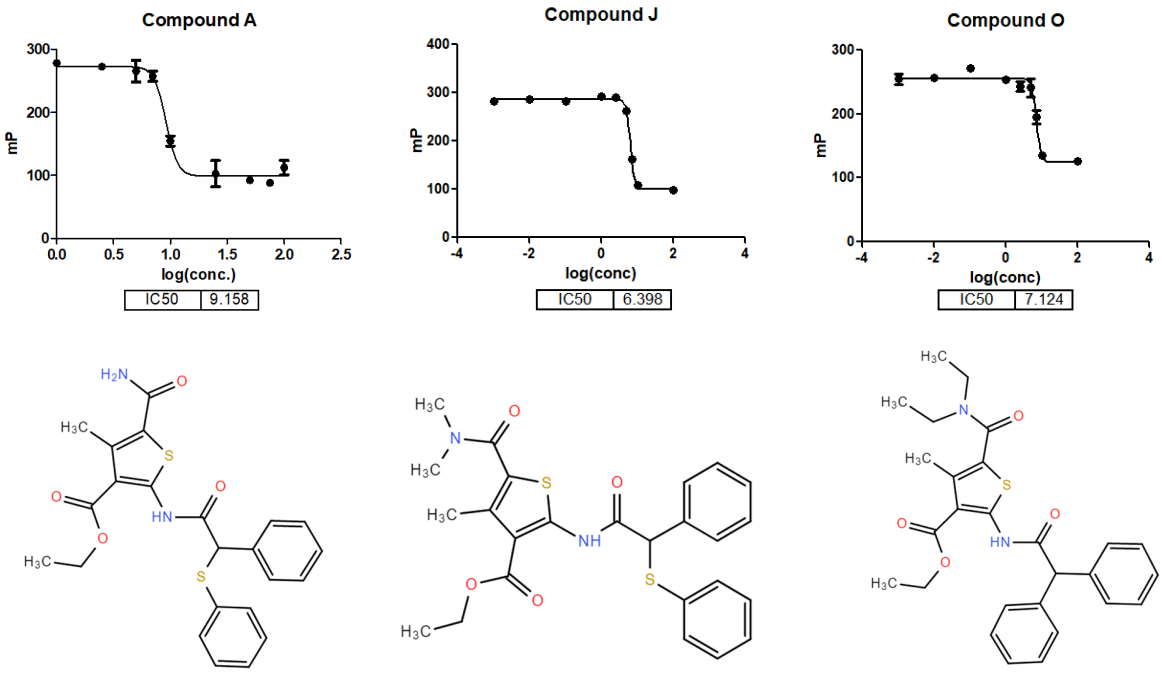

Figure 9: Summary of concentration-dependent disruption of the Rev7/Rev3 PPI by the three most potent inhibitors identified from the virtual screen. Data are from a representative experiment performed in triplicate that was repeated at least two separate times.

VI. MTS Cell Proliferation Assay

The MTS assay is used to quantify cell viability and cytotoxicity. It is based on the reduction of the water-soluble tetrazolium salt, MTS compound by NAD(P)H-dependent dehydrogenase enzymes in metabolically active cells (Abcam). MTS reduction generates a colored formazan dye which is quantified by measuring the absorbance at 490 nm. This assay measures the number of viable cells at the time of MTS treatment and is used in this study to determine the compounds' ability to increase cancer cell sensitivity to cisplatin. The MTS assay also tests our hypothesis that Rev7/Rev3 TLS inhibitors do not demonstrate toxicity on their own as they are used as adjuvant agents to cisplatin. We used A2780 cells because they are a clinically relevant model system since ovarian cancer is commonly treated with cisplatin. A2780cisR cells, mutant ovarian cancer cells that survive in low concentrations of cisplatin, were also used to determine if our Rev7/Rev3 inhibitors can decrease cell viability in conjunction with cisplatin and potentially avert chemoresistance.

The 4 combinations, described in the Methods, were performed to compare differences in cell viability across all treatment groups. As expected, cisplatin alone is potent at inhibiting cell viability in A2780 cells (GI50 26.37 μM) and A2780cisR cells (GI50 79.34 μM). The higher GI50 value for A2780cisR cells confirms cellular resistance to cisplatin as a higher dose of cisplatin needs to be added to cause 50% cell viability. (**Figure 10**) None of the three Rev7/Rev3 inhibitors were as potent as cisplatin at inhibiting cell viability as demonstrated by the lack of concentration-dependent cell death. In fact, cells treated with Compounds J and O alone showcased increased cellular viability at higher concentrations. (**Figure 10**)

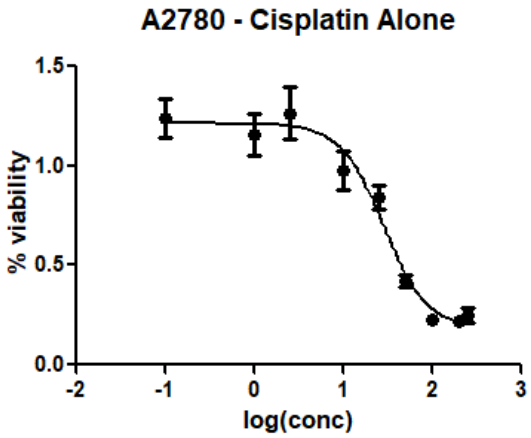

GI50 = 28.37

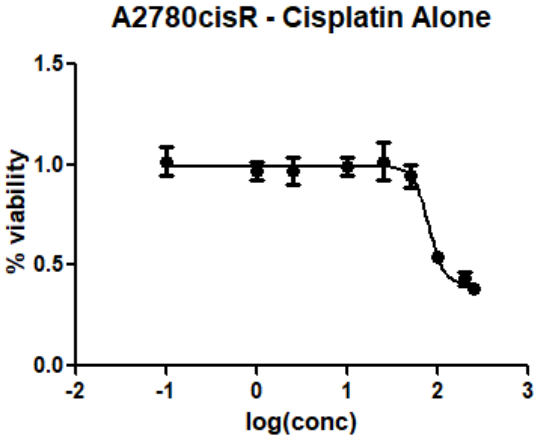

GI50 = 79.34

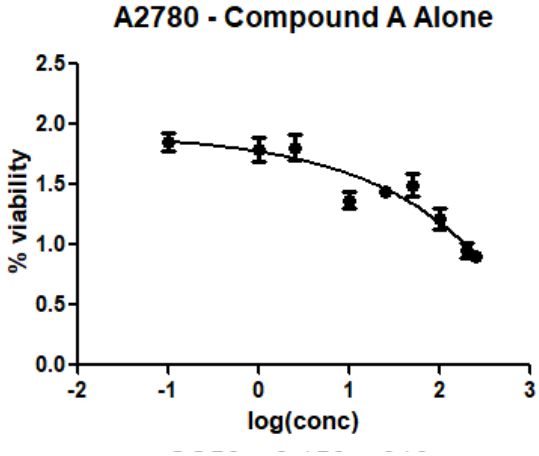

GI50 = 3.159e+010

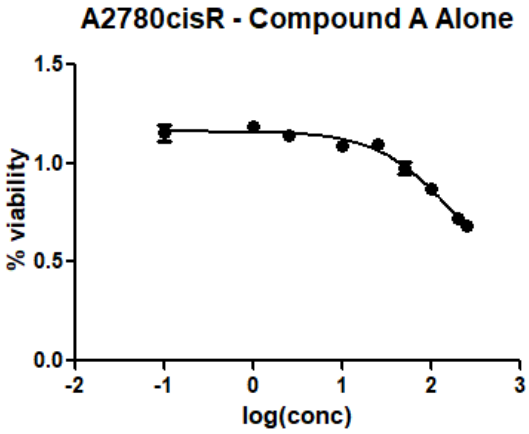

GI50 = 157.9

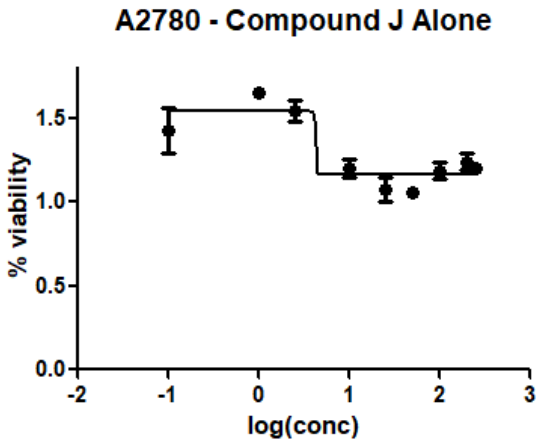

GI50 = 4.243

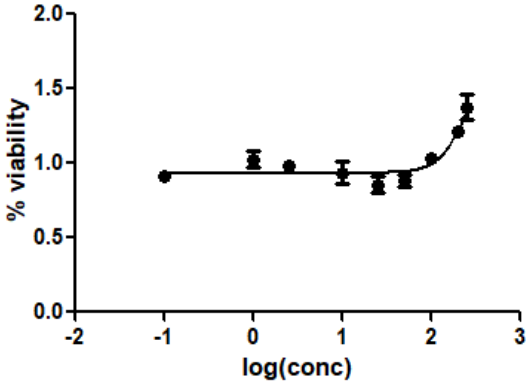

GI50 = 296.2

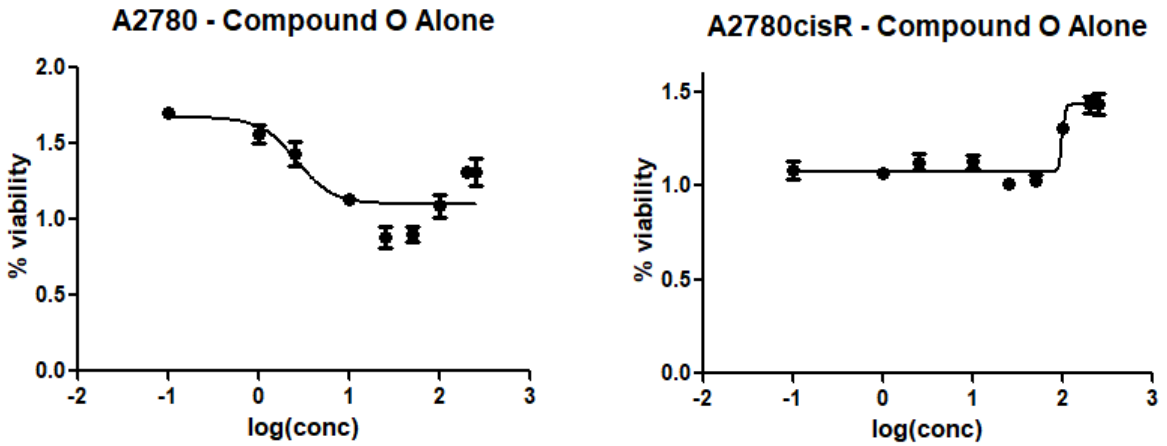

GI50 = 2.646 GI50 = 97.37

Figure 10: Cell viability graphs of A2780 and A2780cisR ovarian cancer cells treated with cisplatin and Rev7/Rev3 inhibitors alone. GI50 values were calculated through nonlinear regression in GraphPad Prism.

Once it was confirmed that the Rev7/Rev3 inhibitors were not toxic to the cells, we tested for synergistic interactions. These interactions are ideal because they allow the use of lower doses of the combination constituents, a therapy that may reduce toxic side effects commonly associated with chemotherapy. Both cell lines treated with a combination cocktail of either 1 μM or 10 μM of Rev7/Rev3 inhibitor with varying concentrations of cisplatin showed increased resistance to the treatment. (**Figure 11**) These results demonstrate that Rev7/Rev3 TLS inhibitors do not synergize with cisplatin which means that coadministration of both drugs does not enhance cisplatin sensitivity and cancer cell death.

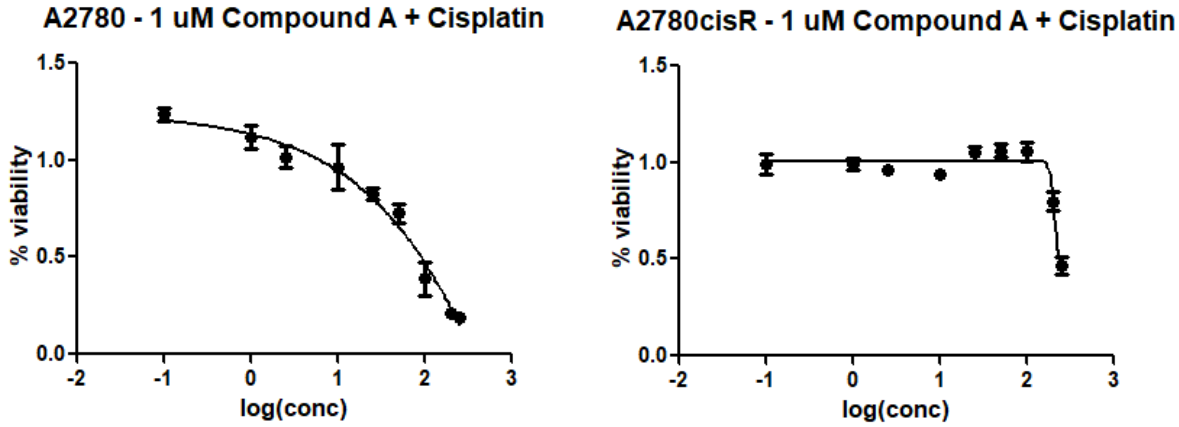

GI50 = 5369 GI50 = 206.4

A2780 - 10 uM Compound A + Cisplatin

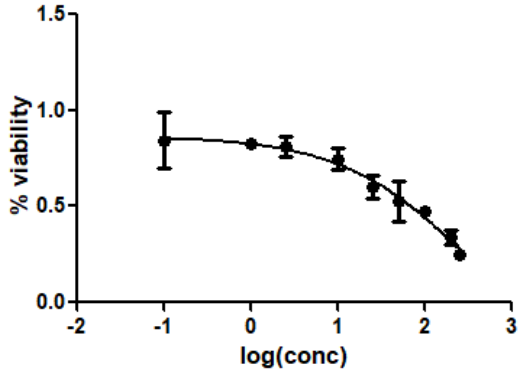

GI50 = 360.6

A2780cisR - 10 uM Compound A + Cisplatin

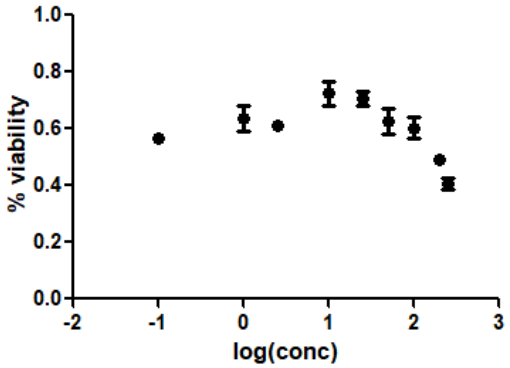

Not Converged

A2780 - 1 uM Compound J + Cisplatin

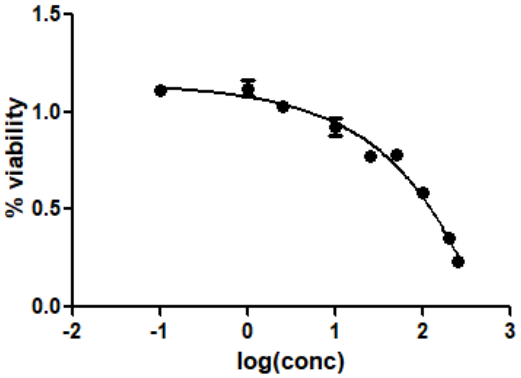

GI50 = 9.812e+008

A2780cisR - 1 uM Compound J + Cisplatin

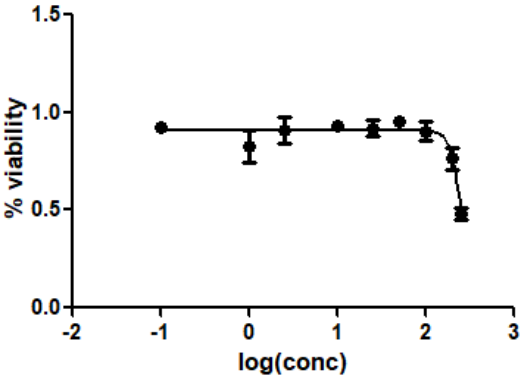

GI50 = 274.1

A2780 - 10 uM Compound J + Cisplatin

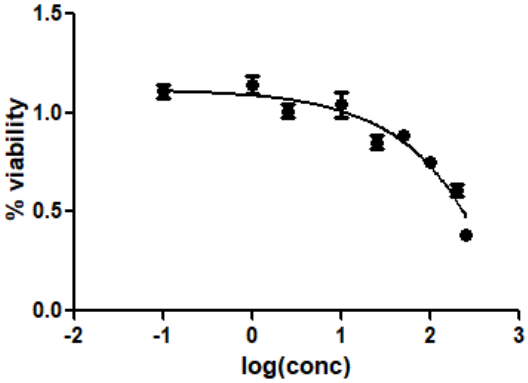

GI50 = 1.236e+008

A2780cisR - 10 uM Compound J + Cisplatin

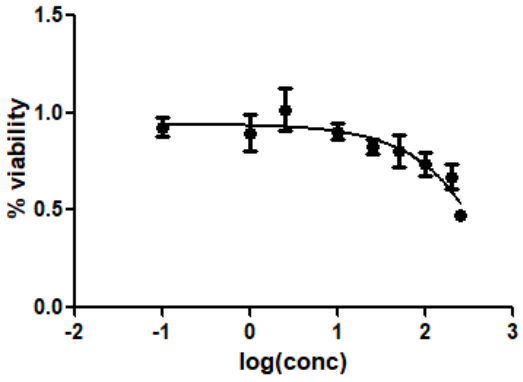

GI50 = 367839

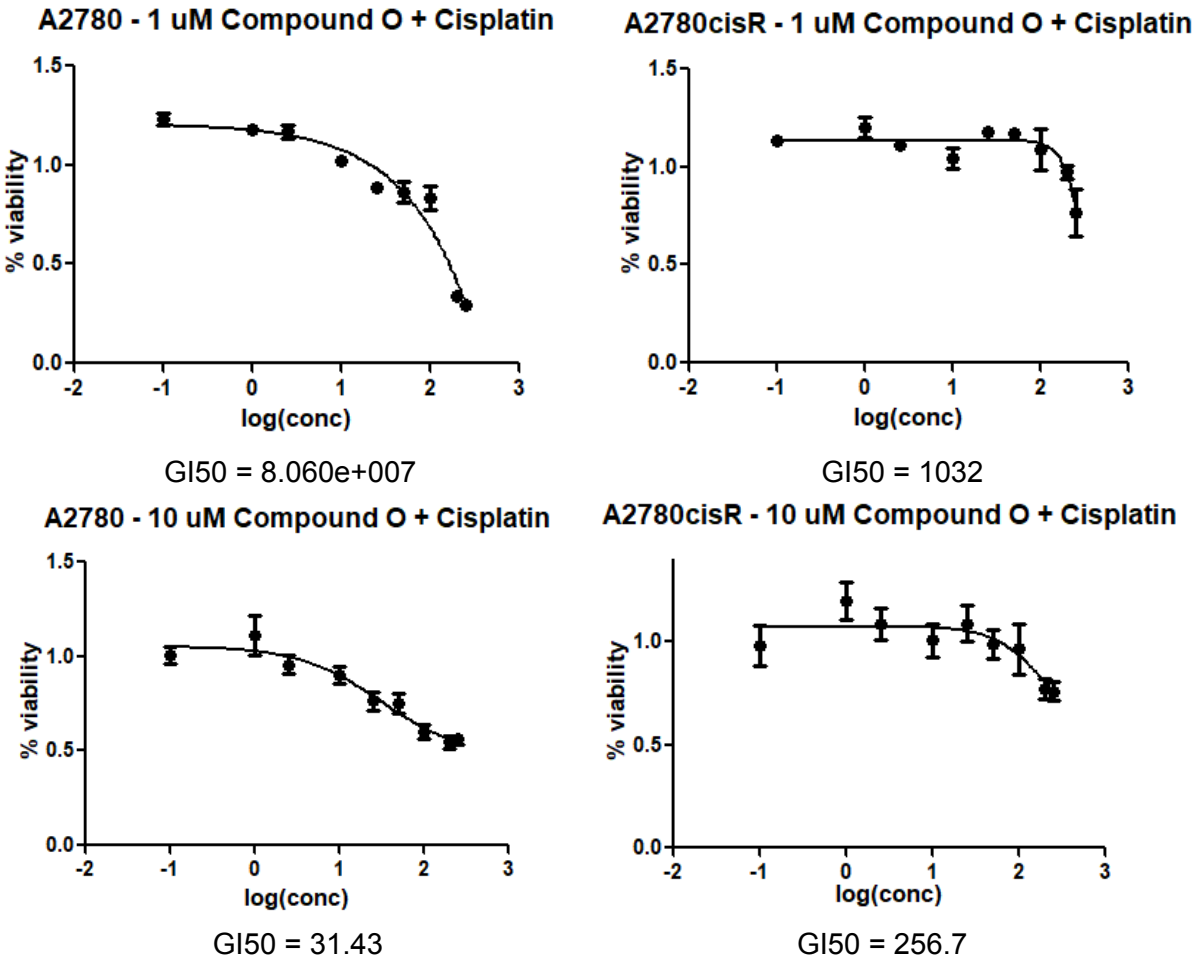

Figure 11: Rev/Rev3 inhibitors do not enhance cancer cell sensitivity to cisplatin. Cell viability graphs of A2780 and A2780cisR ovarian cancer cells treated with either 1 μM or 10 μM of Rev7/Rev3 inhibitor in combination with varying concentrations of cisplatin. GI50 values for each of these time points were calculated through nonlinear regression in GraphPad Prism.

Compound	GI50 of Compound Alone	GI50 of Cisplatin + 1 μM Compound	GI50 of Cisplatin + 10 μM Compound
Cisplatin	19.62 ± 12.37	ND	ND
A	1.58E+10 ± 2.23E+10	5369	360.6
J	6.71 ± 3.49	9.81E+08	1.24E+08
O	2.88 ± 0.33	8.06E+07	31.43

Table 3: Summary of GI50 values (μM) after treatment with cisplatin and TLS inhibitor candidates in A2780 cells. Data are from experiments performed in triplicate with some repeated two separate times.

Compound	GI50 of Compound Alone	GI50 of Cisplatin + 1 μM Compound	GI50 of Cisplatin + 10 μM Compound
Cisplatin	64.99 ± 20.29	ND	ND
A	94.67 ± 89.43	206.4	Data not converged
J	245.65 ± 71.49	274.1	3.68E+05
O	94.64 ± 3.87	1032	256.7

Table 4: Summary of GI50 values (μM) after treatment with cisplatin and TLS inhibitor candidates in A2780cisR cells. Data are from experiments performed in triplicate with some repeated two separate times.

Discussion

TLS is a major mechanism utilized by cancer cells to bypass DNA lesions produced by first-line genotoxic agents. It promotes chemoresistance by increasing the rate of unrepaired mutations. A combination treatment that includes a TLS inhibitor can be a promising strategy to sensitize cells to chemotherapeutics and even reduce toxic side effects often associated with patients managed on platinating agents. To inform our virtual screen, we performed computational studies to determine the key amino acids required for the Rev7 and Rev3 protein-protein interactions (PPI). Our results demonstrated that the antiparallel β sheet of both RBM1 and RBM2 peptides was essential for key interactions with Rev7. Therefore, during our virtual screen, we selected ligands/compounds that docked against the βRBM region. Conformation stability of both RBM peptides was validated with experimental IC50 values, which showed that RBM1 had a slightly higher binding affinity for Rev7, though this was non-significant.

Using computational methods to perform a virtual screen, we identified 9 hit compounds with the potential to disrupt the Rev7/Rev3 PPI. These compounds were then tested in an optimized *in vitro* fluorescence polarization (FP) assay which led to the discovery of Compound A as the most potent inhibitor. Pharmacophore derivatives of Compound A (Compounds J and O) were also tested in the same FP assay to further elucidate the Rev7/Rev3 binding pocket. A robust, colorimetric cell survival experiment called the MTS assay was then employed to build upon the *in vitro* results obtained from the FP assay. The MTS data demonstrates that both cell lines are not as sensitive to treatment with Rev7/Rev3 inhibitors as they are with cisplatin. This confirmed that our inhibitors are not toxic and can be used as potential adjuvant agents. An unusual finding from this experiment is that at concentrations greater than 100 μM, both cell lines became more resistant to high doses of the inhibitors.

In the MTS combination studies, none of the three inhibitors provided the expected additional inhibitory effects on cell proliferation at either 10 μM or 1 μM. These results indicate that synergistic interactions do not take place between cisplatin and our Rev7/Rev3 inhibitors and that disrupting the Rev7/Rev3 pocket of polζ may not be as promising as targeting other key TLS domains such as Rev1-CT and the Rev1-interaction region (Sail, 2017; Dash, 2019). Future work can focus on optimizing the chemical structure of the compounds identified in this study to better understand their interactions within the Rev7/Rev3 domain. As previously

mentioned in the Introduction, studies have shown that inhibiting Rev7 and Rev3 function increases cancer cell sensitivity to cisplatin. Therefore, it is worth developing synergizing inhibitors that target either the PPI that holds the two domains together, individually disrupting hey interactions within either domain, or altogether targeting another domain within polζ.

References

Dash, Radha Charan, and Kyle Hadden. “Protein-Protein Interactions in Translesion Synthesis.” *Molecules (Basel, Switzerland)* vol. 26,18 5544. 13 Sep. 2021, doi:10.3390/molecules26185544

Friedberg, Errol C. “DNA damage and repair.” *Nature* vol. 421,6921 (2003): 436-40. doi:10.1038/nature01408

Truong, Judy, et al. “The impact of pricing strategy on the costs of oral anti-cancer drugs.” Cancer medicine vol. 8,8 (2019): 3770-3781. doi:10.1002/cam4.2269

Brown, Andrea et al. “Cisplatin-Based Chemotherapy of Human Cancers.” *Journal of cancer science & therapy* vol. 11,4 (2019): 97.

Dmitry Korzhnev and M. Kyle Hadden “Targeting the Translesion Synthesis Pathway for the Development of Anti-Cancer Chemotherapeutics” Journal of Medicinal Chemistry 2016 59 (20), 9321-9336 DOI: 10.1021/acs.jmedchem.6b0059

Pustovalova, Yulia et al. “The C-terminal domain of human Rev1 contains independent binding sites for DNA polymerase η and Rev7 subunit of polymerase ζ.” FEBS letters vol. 586,19 (2012): 3051-6. doi:10.1016/j.febslet.2012.07.021

Rizzo, Alessandro A et al. “Rev7 dimerization is important for assembly and function of the Rev1/Polζ translesion synthesis complex.” *Proceedings of the National Academy of Sciences of the United States of America* vol. 115,35 (2018): E8191-E8200. doi:10.1073/pnas.1801149115

Wu, Fang et al. “DNA polymerase zeta regulates cisplatin cytotoxicity, mutagenicity, and the rate of development of cisplatin resistance.” *Cancer research* vol. 64,21 (2004): 8029-35. doi:10.1158/0008-5472.CAN-03-3942

Gan, Gregory N et al. “DNA polymerase zeta (pol zeta) in higher eukaryotes.” *Cell research* vol. 18,1 (2008): 174-83. doi:10.1038/cr.2007.117

Doles J, Oliver TG, Cameron ER, et al. Suppression of Rev3, the catalytic subunit of Polζ, sensitizes drug-resistant lung tumors to chemotherapy. Proc Natl Acad Sci U S A. 2010;107:20786-20791.

Sakurai Y, Ichinoe M, Yoshida K, et al. Inactivation of REV7 enhances chemosensitivity and overcomes acquired chemoresistance in testicular germ cell tumors. Cancer Lett. 2020;489:100-110.

Actis, Marcelo L et al. “Identification of the first small-molecule inhibitor of the REV7 DNA repair protein interaction.” *Bioorganic & medicinal chemistry* vol. 24,18 (2016): 4339-4346. doi:10.1016/j.bmc.2016.07.026

K. McNally, J.A. Neal, T.P. McManus, J.J. McCormick, V.M. Maher
hRev7, putative subunit of hPolζ, plays a critical role in survival, induction of mutations, and progression through S-phase, of UV(254nm)-irradiated human fibroblasts
DNA Repair, 7 (2008), pp. 597-604

MTS Assay Kit (Cell Proliferation) (Colorimetric) (AB197010).” *Abcam*, https://www.abcam.com/mts-assay-kit-cell-proliferation-colorimetric-ab197010.html#:~:text=The%20MTS%20assay%20is%20used,soluble%20in%20call%20culture%20media.

Sail, Vibhavari et al. “Identification of Small Molecule Translesion Synthesis Inhibitors That Target the Rev1-CT/RIR Protein-Protein Interaction.” *ACS chemical biology* vol. 12,7 (2017): 1903-1912. doi:10.1021/acschembio.6b01144

Dash, Radha C et al. “Virtual Pharmacophore Screening Identifies Small-Molecule Inhibitors of the Rev1-CT/RIR Protein-Protein Interaction.” *ChemMedChem* vol. 14,17 (2019): 1610-1617. doi:10.1002/cmdc.201900307